



Transcriptome profiling of kisspeptin neurons from the mouse arcuate nucleus reveals new mechanisms in estrogenic control of fertility

Balázs Göcz^{a,b,1}, Éva Rimpler^a, Miklós Sárvári^a, Katalin Skrapits^a, Szabolcs Takács^a, Imre Farkas^a, Veronika Csillag^c, Sarolta H. Trinh^a, Zsuzsanna Bardóczy^d, Yvette Ruska^e, Norbert Solymosi^{f,g}, Szilárd Póliska^h, Zsuzsanna Szőkeⁱ, Lucia Bartoloni^j, Yassine Zouaghi^j, Andrea Messina^l, Nelly Pitteloud^{j,k}, Ross C. Anderson^l, Robert P. Millar^l, Richard Quinton^{m,n}, Stephen M. Manchisi^o, William H. Colledge^a, and Erik Hrabovszky^{a,1}

Edited by Donald Pfaff, The Rockefeller University, New York, NY; received July 30, 2021; accepted May 5, 2022

Kisspeptin neurons in the mediobasal hypothalamus (MBH) are critical targets of ovarian estrogen feedback regulating mammalian fertility. To reveal molecular mechanisms underlying this signaling, we thoroughly characterized the estrogen-regulated transcriptome of kisspeptin cells from ovariectomized transgenic mice substituted with 17 β -estradiol or vehicle. MBH kisspeptin neurons were harvested using laser-capture microdissection, pooled, and subjected to RNA sequencing. Estrogen treatment significantly (*p*.adj. < 0.05) up-regulated 1,190 and down-regulated 1,139 transcripts, including transcription factors, neuropeptides, ribosomal and mitochondrial proteins, ion channels, transporters, receptors, and regulatory RNAs. Reduced expression of the excitatory serotonin receptor-4 transcript (*Htr4*) diminished kisspeptin neuron responsiveness to serotonergic stimulation. Many estrogen-regulated transcripts have been implicated in puberty/fertility disorders. Patients (*n* = 337) with congenital hypogonadotropic hypogonadism (CHH) showed enrichment of rare variants in putative CHH-candidate genes (e.g., *LRP1B*, *CACNA1G*, *FNDC3A*). Comprehensive characterization of the estrogen-dependent kisspeptin neuron transcriptome sheds light on the molecular mechanisms of ovary–brain communication and informs genetic research on human fertility disorders.

fertility | gene expression | neuropeptides | reproduction | RNA sequencing

Endocrine homeostasis depends on the complex interplay between the hypothalamus and the pituitary and peripheral endocrine organs. Gonadotropin-releasing hormone (GnRH)-synthesizing neurons constitute the final output conduit from the hypothalamus for the control of reproduction (1, 2). The neurosecretory axons of these neurons terminate in the external zone of the median eminence. Episodic release of GnRH at this site into the hypothalamic-hypophysial portal circulation system evokes pulsatile luteinizing hormone (LH) and follicle-stimulating hormone secretion from the anterior pituitary, which, in turn, stimulates gametogenesis and sex steroid synthesis in the male and female gonads. In both sexes, gonadal steroids inhibit the hypothalamic-pituitary-gonadal axis via homeostatic negative feedback to the hypothalamus and the anterior pituitary. In females, rising blood levels of ovarian estrogen hormones at the late follicular phase of the reproductive cycle cause a switch from negative to positive feedback. This rise is a key signal for the midcycle GnRH/LH surge, which triggers ovulation (1, 2).

Hypothalamic peptidergic neurons synthesizing kisspeptin (KP) express estrogen receptor- α (ER α) and play crucial roles in mediating the positive and negative estrogen feedback to GnRH neurons via KP/KP receptor signaling. In rodents, KP neurons located in the rostral periventricular area of the third ventricle (RP3V; also referred to as the KP neuron population of the anteroventral periventricular nucleus) are critically involved in the induction of preovulatory GnRH/LH surges during positive feedback. The arcuate nucleus (ARC) in the mediobasal hypothalamus (MBH) contains an additional large KP neuron population. This anatomical region has long been known as a critical feedback site in the communication between the ovary and the hypothalamus. In postmenopausal women, absence of estrogen feedback causes profound morpho-functional changes within this region, characterized by neuronal hypertrophy (3) and increased neurokinin B (NKB) (4, 5), KP (5, 6), and substance P (4, 7) biosynthesis. In various mammals, KP neurons of the ARC (aka KNDy neurons) coexpress KP, NKB, and dynorphin. Growing evidence suggests that ARC KNDy neurons are key players in negative estrogen feedback (2, 8), and their KP output also regulates the pattern of pulsatile GnRH/LH secretion (9).

Significance

The arcuate nucleus (ARC) of the mediobasal hypothalamus is critically involved in hormonal communication from ovary to brain. Negative estrogen feedback to kisspeptin synthesizing neurons of the ARC is a crucial determinant of hypothalamic gonadotropin-releasing hormone secretion regulating fertility. We performed deep transcriptome profiling of ARC kisspeptin neurons with RNA sequencing and identified over 2,000 estrogen-sensitive transcripts. Several genes responding to estrogen treatment in ovariectomized mice exhibited rare variants in a patient database with pubertal defects and emerge as candidate genes for a role in puberty/fertility disorders. Comprehensive characterization of the estrogen-dependent kisspeptin neuron transcriptome in mice has important clinical implications for the hypothalamic regulation of human menstrual cycle and for the putative molecular consequences of postmenopausal estrogen deficiency.

The authors declare no competing interest.

This article is a PNAS Direct Submission.

Copyright © 2022 the Author(s). Published by PNAS. This article is distributed under Creative Commons Attribution-NonCommercial-NoDerivatives License 4.0 (CC BY-NC-ND).

¹To whom correspondence may be addressed. Email: gocz.balazs@koki.hu or hrabovszky.erik@koki.hu.

This article contains supporting information online at <http://www.pnas.org/lookup/suppl/doi:10.1073/pnas.2113749119/-DCSupplemental>.

Published June 28, 2022.

A recent RNA sequencing (RNA-seq) study successfully used the RiboTag technology to selectively isolate actively translated messenger RNAs (mRNAs) from RP3V KP neurons. In this elegant work, hundreds of transcripts showed differential expression between ovariectomized (OVX) mice with and without 17 β -estradiol (E2) substitution; these transcripts may play important roles in estrogen positive feedback (10).

Detailed information about the estrogen-dependent transcripts and biological processes of the ARC and its KP (KNDy) neuron population involved in negative feedback is currently unavailable.

In this study, we characterize the estrogen-dependent transcriptome of the mouse ARC and its KP neurons with RNA-seq. Using tissue samples isolated with laser-capture microdissection (LCM) from OVX mice subjected to a chronic 4-d E2 treatment, we identify thousands of genes regulated by estrogen in the ARC and, specifically, in its KP cell population. We confirm with slice electrophysiology that the E2-induced transcriptional changes of serotonin receptor isoforms influence KP neuron responsiveness to serotonin. Based on the observation that many E2-regulated transcripts we identified were previously implicated in human puberty/fertility disorders, we propose a strategy to discover disease genes using the list of the most heavily E2-dependent KP neuron transcripts. Indeed, burden analysis of such genes can reveal significant enrichment of rare transcript variants in patients with congenital hypogonadotropic hypogonadism (CHH).

Results

E2 Treatment of OVX Mice Results in High Physiological Serum E2 Levels and Robust Uterine Hypertrophy. Estrogen-regulated transcripts were investigated in surgically OVX mice receiving a 4-d E2 substitution (OVX+E2) from a subcutaneous capsule implant (SI Appendix, Fig. S1A). This treatment produced a 7.59 ± 0.7 pg/mL (mean \pm SEM) serum E2 concentration in test animals ($n = 4$), which falls within the physiological range in cycling female mice (~ 6 pg/mL in diestrus and ~ 8 pg/mL in proestrus) (11) and exerts strong negative feedback on the neuroendocrine hypothalamus. The biological response of the OVX mice to the 4-d E2 treatment was confirmed by a robust increase in uterine weight (136.5 ± 11.8 mg of OVX+E2 animals; $n = 6$ vs. 18.0 ± 0.4 mg of OVX+Veh controls; $n = 6$; $P = 6.3E-07$).

The Laser-Microdissected ARC Provides High-Quality RNA for Deep Transcriptome Profiling. An optimized protocol developed for deep transcriptome profiling of the ARC is shown in SI Appendix, Fig. S1A. This hypothalamic nucleus was readily recognized in Nissl-stained coronal sections. Laser-microdissected tissues collected and pooled proportionally from the rostral, middle, and caudal ARC of OVX+E2 ($n = 6$) and OVX+Veh ($n = 5$) mice provided sources for well-preserved RNA (RNA integrity number: 7.1-8.2). Sequencing of the RNA-seq libraries with the Illumina NextSeq 500/550 High Output (v2.5) kit generated 22.6 M reads as an average from the 11 cDNA libraries. Reads were mapped to the mouse reference genome with a mean overall alignment rate of 86.8%. Gene level quantification of read counts was performed by featureCounts, and 89.1% of mapped reads were assigned to genes.

Bioinformatic Analysis Identifies 1,157 Up-Regulated and 960 Down-Regulated Transcripts in the ARC of Chronically E2-Treated OVX Mice. The 2,117 estrogen-regulated transcripts ($p_{adj.} < 0.05$) showed conspicuous sample homogeneity

among animals of the same treatment group. The ARC of OVX+E2 mice contained 1,157 up-regulated (fold change [FC] > 1) and 960 down-regulated (FC < 1) transcripts (SI Appendix, Fig. S1B). In total, 235 transcripts exhibited a $|\log_2FC|$ above 1.0. The top changes in each direction are shown in SI Appendix, Fig. S2A. The full list of the 2,117 estrogen-regulated transcripts and their functional categories defined based on multiple online databases and methods are provided in Dataset S1. Categorized transcripts were related to autophagy ($n = 115$), ubiquitination ($n = 37$) and encoded neuropeptides or neuropeptide-associated proteins ($n = 20$), miscellaneous ion channels ($n = 42$), transporters ($n = 83$), classical receptors ($n = 30$), other receptors ($n = 136$), ribosomal proteins ($n = 21$), transcription factors ([TFs] $n = 104$), long noncoding RNAs (lncRNAs; $n = 40$), and microRNAs (miRNAs; $n = 9$). The list also included predicted protein coding genes ($n = 17$) and other predicted genes ($n = 83$) with unknown functions. Genes regulated by E2 in the ARC were known to be expressed in multiple cell types (e.g., *Esr1*, *Ar*, *Pgr*, *Ghsr*), unknown cell types (e.g., *Aqp5*, *Drd1*, *Sstr1-3*, *Htr4*), and non-KP neurons (e.g., *Agrp*, *Sst*, *Cartpt*, *Slc6a3*, *Nts*), in addition to a large set found enriched in KP neurons in earlier Drop-seq analyses (e.g., *Tac2*, *Nhlh2*, *Pdyn*, *Prhr*, *Nr5a2*, *Tmem35a*, *Rasd1*, *Nr4a2*, *Tacr3*, *Sox14*, *Oprk1*, *Kiss1*) (SI Appendix, Fig. S2B) (12, 13).

ORA Detects 47 Functional Pathways Altered by E2 Treatment in the ARC. Overrepresentation analysis (ORA) identified 47 functional KEGG (Kyoto Encyclopedia of Genes and Genomes) pathways that were altered significantly in response to E2. The highest number of changing transcripts ($n = 56$) occurred in the neuroactive ligand-receptor interaction KEGG pathway, with changes related to both classic and peptidergic (e.g., orexin [OX], neuropeptide Y [NPY], somatostatin [SST]) neurotransmission (SI Appendix, Fig. S2 C and D and Dataset S1). Given that ORA does not consider the functional connectivity of regulated transcripts, signaling pathway impact analysis (SPIA) was used additionally to predict net changes in selected neurotransmitter functions. Results of SPIA indicated the overall activation of the GABAergic and serotonergic pathways and inhibition of the glutamatergic, cholinergic, and dopaminergic synapse pathways (SI Appendix, Fig. S2D).

RNA-Seq Studies of Fluorescent Neurons Isolated with LCM Provide Insight into the Estrogen-Dependent KP Neuron Transcriptome. Although the ARC hosts multiple estrogen-receptive cell types (12, 13), a large number of genes critical for pubertal development, GnRH/LH pulsatility, and estrogen negative feedback are expressed in KP neurons of this region (e.g., *Kiss1*, *Tac2*, *Tacr3*, and *Esr1*). To shed light specifically on the estrogenic regulation of ARC KP cells, in a second RNA-seq experiment, we compared the transcriptomes of these neurons from OVX+Veh ($n = 3$) and OVX+E2 ($n = 3$) mice. Collection and pooling of 300 fluorescently tagged KP neurons from the ARC of each mouse were performed with LCM from sections of formaldehyde-fixed brains. Total RNA samples were isolated (RIN 4.8 to 6.9), and RNA-seq libraries were prepared with the TruSeq Stranded Total RNA Library Prep Gold kit, as recommended for partly degraded RNA falling into the nanogram range (14). RNA-seq generated 20.5 M reads/sample, as an average. Reads were mapped to the mouse reference genome using the RNA-seq aligner software STAR (Spliced Transcripts Alignment to a Reference; v 2.7.3a), with an average overall alignment rate of 74.9% (SD = 3.5%). Gene level

quantification of read counts based on mouse genome with Ensembl (release 100) annotation was performed by featureCounts (subread v 2.0.0) with a 38.6% mean of mapped reads assigned to genes (SD = 0.9%). The optimized protocol (*SI Appendix*, Fig. S1A) resulted in highly homogeneous blocks within the heat map, with significant ($p_{adj.} < 0.05$) effects of the E2 treatment (*SI Appendix*, Fig. S1C).

Bioinformatic Analysis Identifies 1,190 Up-Regulated and 1,139 Down-Regulated KP Neuron Transcripts in OVX Mice Substituted with E2. The number of KP neuron transcripts that changed significantly ($p_{adj.} < 0.05$) in response to the 4-d E2 treatment was 2,329. Genes with the highest $|\log_2FC|$ values shown in Fig. 1A included many low-to-medium abundance transcripts, which were undetected in earlier Drop-seq studies of hypothalamic cell types (12, 13). In total, 1,442 changes (774 up- and 668 down-regulations) within KP cells exceeded $|\log_2FC|$ 1.0 (Fig. 1B), unlike during the analysis of the whole ARC, where the magnitude of most changes was much smaller (*SI Appendix*, Fig. S2B).

ORA Detects 83 Estrogen-Regulated Functional Pathways in KP Neurons. ORA identified 83 significantly altered KEGG pathways, with the highest numbers of changing genes in the ribosome ($n = 57$) and the neuroactive ligand-receptor interaction ($n = 57$) functional pathways (Fig. 1C and D and Dataset S2). Use of SPIA indicated overall activation of the GABAergic and glutamatergic synapse pathways and overall inhibition of the cholinergic, dopaminergic, and serotonergic synapse pathways in response to the E2 treatment. Changes in neurotransmitter and neurotransmitter receptor transcripts are presented graphically in Fig. 1D.

Estrogen-Responsive Transcripts of KP Neurons Fall into Various Functional Categories. As in the case of the ARC transcriptome, we used several online databases for the functional classification of estrogen-regulated transcripts. Many E2-regulated genes were related to autophagy ($n = 156$) or ubiquitination ($n = 45$). Others encoded neuropeptides ($n = 15$), miscellaneous ion channels ($n = 46$), transporters ($n = 72$), classical neurotransmitter receptors ($n = 26$), other receptor types ($n = 110$), ribosomal ($n = 60$) and mitochondrial ($n = 37$) proteins, TFs ($n = 109$), lncRNAs ($n = 60$), and miRNAs ($n = 5$). They included predicted protein coding genes ($n = 31$) and a large number of other predicted genes ($n = 192$), in addition to transcripts left uncategorized. Members of selected gene categories are listed in Fig. 2, and all of the significant estrogen-induced changes ($n = 2,329$) are provided in Dataset S2.

The large number of regulated TFs ($n = 109$) likely contributed to secondary transcriptional changes. E2 suppressed mRNA expression of nuclear hormone receptors (*Ar*, *Esr1*), AP-1 TFs (*Fos*, *Fosb*, *Junb*, *Jund*), early growth response proteins (*Egr1*, 3, 4), the neuronal-activity-dependent TF (*Npas4*), orphan nuclear receptors (*Nr4a1*, *Nr4a3*), steroidogenesis regulators (*Crem*), and many zinc finger proteins. Estrogen inhibited the prohormone convertase PC1/3 transcriptional regulator *Creb3l1* and the enzyme (*Pcsk1*) as well. Furthermore, E2 activated mRNA expression of some hormone receptors (*Pgr*, *Thrb*), transcriptional mediator of progesterone synthesis (*Cebpb*), and TFs SOX (*Sox11*, *Sox18*) and STAT (*Stat5a*, *Stat5b*).

Estrogen Regulates Postsynaptic Receptors for Classic and Neuropeptide Neurotransmitters Innervating KP Neurons. A number of neurotransmitter receptors responded to the 4-d E2 treatment. These included the *Htr2a*, *Htr4*, *Htr5a*, and *Htr7* serotonin receptors; the *Npy1r*, *Npy4r*, and *Npy5r* NPY

receptors; the *Sstr2* and *Sstr3* SST receptors; and the *Ox2* OX receptor, among others (Figs. 1D and 2). These changes suggested that the receptor ligands can exert estrogen-dependent afferent control on KP neurons. To provide anatomical support to this notion, a series of dual-immunofluorescence experiments were carried out on ARC sections of OVX+Veh and OVX+E2 KP-Cre/ZsGreen mice. Confocal microscopic analysis demonstrated the presence of the 5-HT marker serotonin transporter (SERT; Fig. 3A), OX B (Fig. 3B), NPY (Fig. 3C), and SST (Fig. 3D) in axosomatic and axodendritic afferents to ARC KP neurons, thus suggesting the potential contribution of these transmitters to the estrogen-dependent neuronal control of KP cells. As clear differences in innervation patterns were not noticed between the two animal models, the number of contacts was not analyzed quantitatively. To confirm that SSTergic fibers provide synaptic input to KP neurons, dual-label immuno-electron microscopy was used. This study established that SST-immunoreactive fibers establish synaptic contacts on KP dendrites (Fig. 3E) and cell bodies (Fig. 3F). Similar ultrastructural evidence for serotonin, NPY, and OX containing synapses onto KP cells is currently unavailable. Antibodies used in anatomical studies are specified in *SI Appendix*, Table S1.

Estrogenic Regulation of Serotonergic Receptors Correlates with Reduced Excitatory Responses of KP Neurons to Low Doses of 5-HT and the 5-HT4R AG Cisapride. The serotonergic system has emerged as an important mediator of leptin (15) and estrogen (16) effects on reproduction. Four distinct serotonin receptors showed robust estrogenic regulation within KP neurons; the inhibitory *Htr5a* was up-regulated, and the excitatory *Htr2a*, *Htr4*, and *Htr7* isoforms were all down-regulated in E2-treated mice (Fig. 4A and Dataset S2). We hypothesized that these changes cause reduced KP neuron responsiveness to 5-HT stimulation in OVX+E2 mice. Whole-cell patch-clamp electrophysiology was carried out in ARC KP neurons from brain slices of OVX+Veh and OVX+E2 KP-Cre/ZsGreen mice (Fig. 4B). A holding current of +10 pA was used to evoke action potentials in KP neurons, most of which (~94%) are silent in OVX mice (17). Notably, 1,000 nM 5-HT increased the mean firing rate of KP neurons similarly in the OVX+E2 ($266.1 \pm 14.06\%$ of ctrl) and the OVX+Veh ($267.9 \pm 12.69\%$ of ctrl) models. The medium 5-HT dose that we used (200 nM) produced a significantly higher response in OVX+Veh mice ($210.4 \pm 10.34\%$ of ctrl) than in OVX+E2 mice ($157.9 \pm 20.76\%$ of ctrl), whereas the lowest applied dose (100 nM) increased the mean firing frequency in OVX+Veh ($163.6 \pm 6.10\%$ of ctrl) but not in OVX+E2 ($99.5 \pm 6.60\%$ of ctrl) animals (Fig. 4C and D). Preincubation of slices with the selective 5-HT4R antagonist (ANT) SB204070 (13 μ M) blunted this response ($123.4 \pm 4.14\%$ of OVX+Veh ctrl), indicating that the 5-HT4R receptor isoform has a major contribution to the effect of 5-HT (Fig. 4D). The highest 100- μ M dose of the selective 5-HT4R agonist (AG) Cisapride stimulated KP neurons equally in the OVX+E2 ($388.6 \pm 17.12\%$ of ctrl) and OVX+Veh ($394.7 \pm 20.64\%$ of ctrl) models. The magnitude of response to a medium dose (10 μ M) was significantly higher in OVX+Veh ($277.2 \pm 13.18\%$ of ctrl) than in OVX+E2 ($175.6 \pm 22.95\%$ of ctrl) mice, whereas 1 μ M Cisapride (the lowest dose having an effect in pilot studies) raised the mean firing frequency of KP cells in the OVX+Veh ($184.1 \pm 13.64\%$ of ctrl) but not in the OVX+E2 ($116.6 \pm 10.06\%$ of ctrl) model (Fig. 4E and F). Cisapride acted selectively on 5-HT4R because its effect was eliminated in the presence of 13 μ M SB204070 (Fig. 4F). The action was direct because 1) it was maintained in the

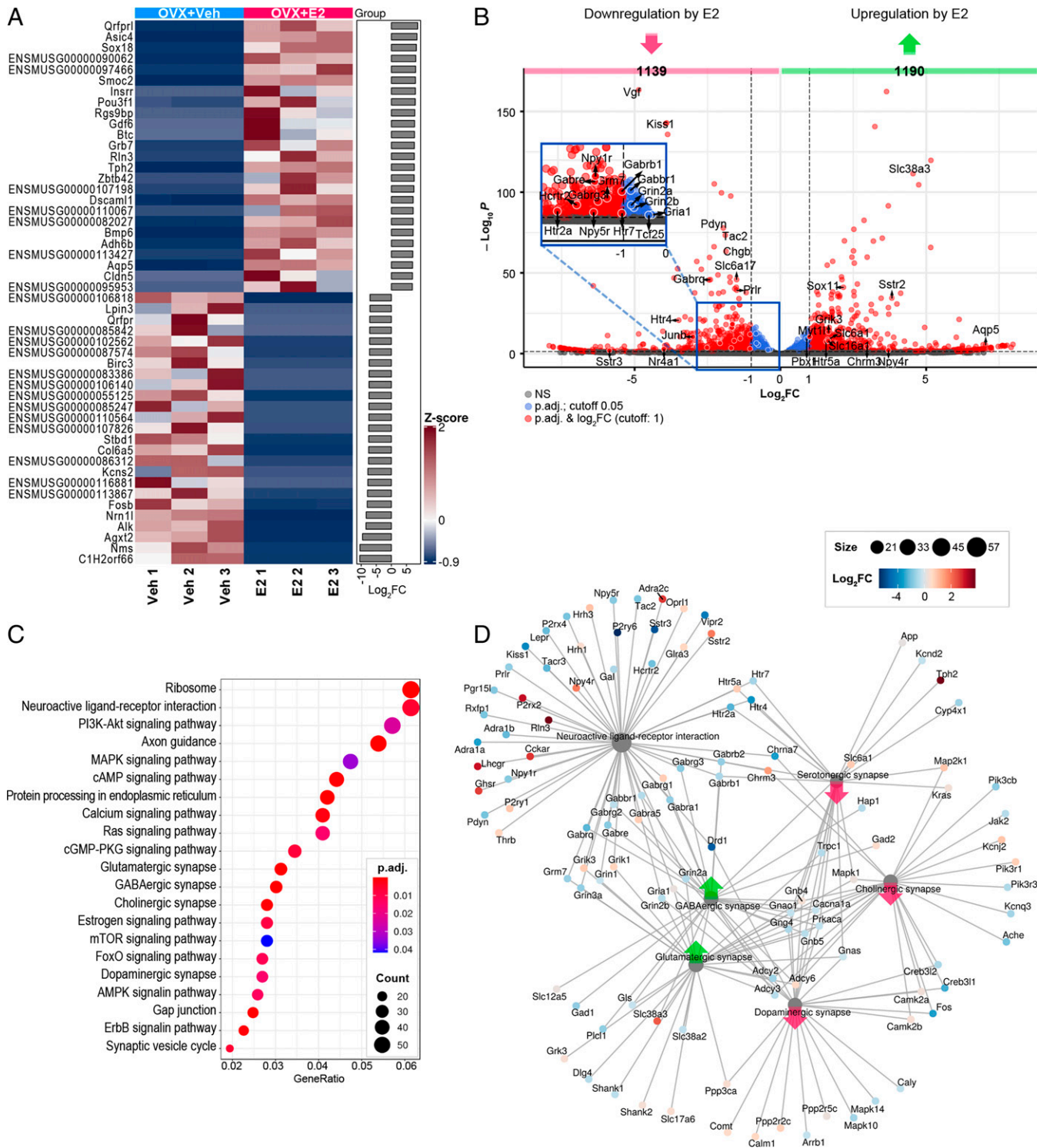


Fig. 1. E2 treatment of OVX mice causes profound transcriptomic changes within KP neurons of the ARC. (A) Heat map of the 25 most down-regulated (*Bottom*) and most up-regulated (*Top*) genes (arranged by FC shown in the gray bar chart) mostly includes transcripts that were previously unreported in KP neurons. (B) Volcano plot reveals a large number of regulatory changes (1,442) that exceed $|\log_2FC| > 1.0$ (red dots), in contrast to the mostly small E2-induced changes typical for the entire ARC region (*SI Appendix, Fig. S2B*). (C) ORA detects 83 significantly altered functional (KEGG) pathways, from which the most relevant 21 are shown in the dot plot. Significant changes happen to the neuroactive ligand-receptor interaction, GABAergic, glutamatergic, cholinergic, and dopaminergic synapse pathways, among others. (D) The altered neurotransmitter and transmitter receptor profiles of KP cells reveal the involvement of multiple neurotransmitters in the estrogen-dependent control of KP neuron functions. SPIA suggests overall activation of the GABAergic and glutamatergic synapse pathways and inhibition of the cholinergic, dopaminergic, and serotonergic synapse pathways. See also [Dataset S2](#).

presence of the ionotropic glutamate and GABA_A receptor inhibitors kynurenic acid (KYN; 2 mM) and picrotoxin (PIC; 100 μ M), respectively, and 2) it was absent if the intracellular solution was supplemented with the membrane impermeable G protein inhibitor guanosine 50-[β -thio] diphosphate (GDP- β -S;

2mM) (Fig. 4F). The higher responsiveness of the OVX+Veh model to low doses of 5-HT and Cisapride supported the notion that estrogenic regulation of the 5-HT receptor isoforms reduces the sensitivity of KP cells to the stimulatory serotonergic input in OVX+E2 mice.

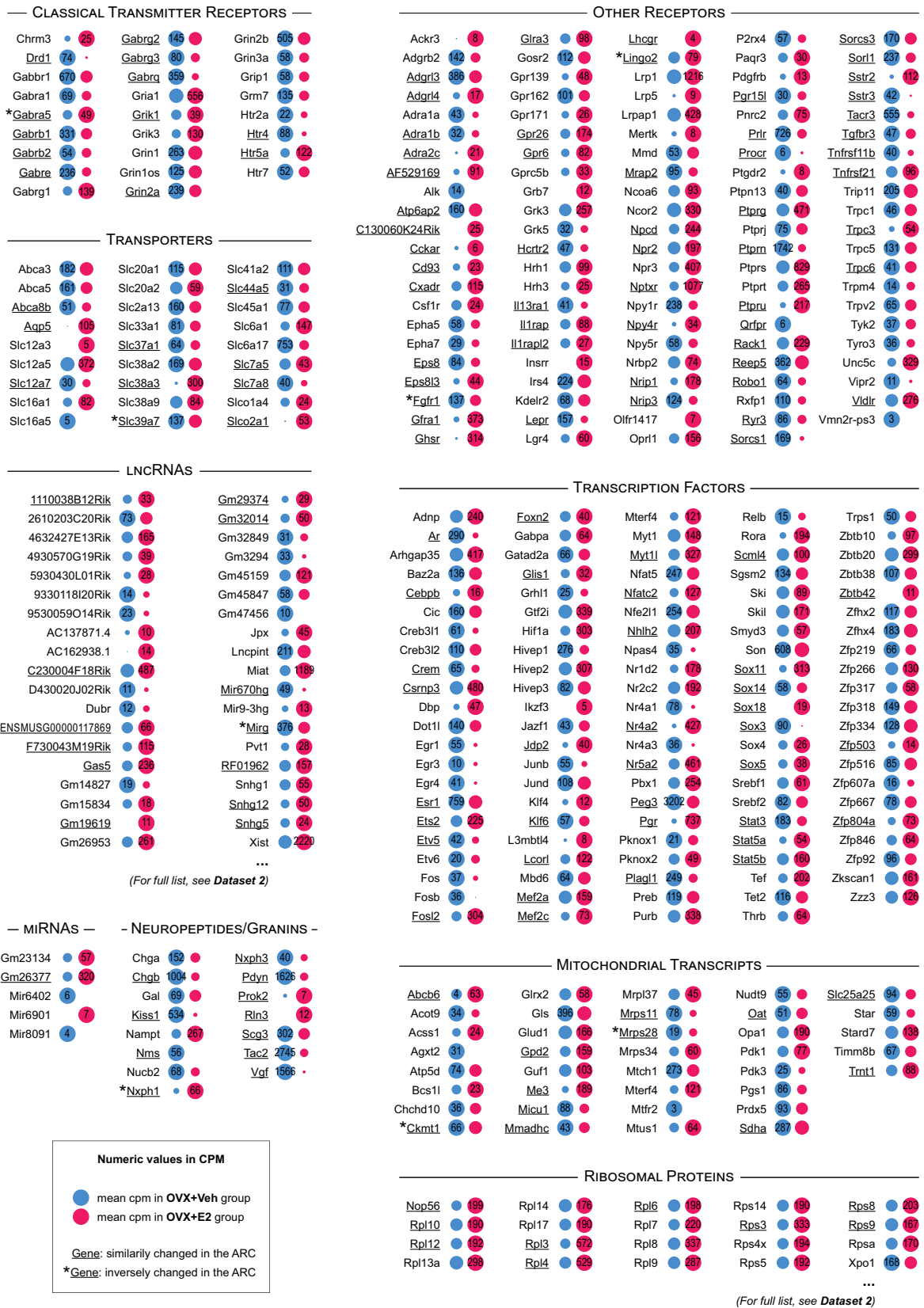


Fig. 2. Estrogen-regulated KP neuron transcripts fall into diverse functional categories. E2-regulated transcripts of ARC KP neurons were categorized based on function using online databases. Many of these transcripts are related to autophagy ($n = 156$) and ubiquitination ($n = 45$). They encode neuropeptides ($n = 15$), miscellaneous ion channels ($n = 46$), transporters ($n = 72$), classical neurotransmitter receptors ($n = 26$), other receptor types ($n = 110$), ribosomal ($n = 60$) and mitochondrial ($n = 37$) proteins, TFs ($n = 109$), lncRNAs ($n = 60$), and miRNAs ($n = 5$). They include predicted protein coding genes ($n = 31$) and a large number of other predicted genes ($n = 192$). Dataset S2 contains the full list of E2-regulated KP neuron transcripts and a more detailed functional categorization. Genes that also show significant E2-dependent regulation in the ARC are underlined. Asterisks indicate inverse regulatory changes in the ARC region and in KP neurons, whereas all other genes changed significantly ($p_{adj.} < 0.05$) only in KP neurons. Numbers in dots reflect transcript abundances in CPM units. Dot areas change in proportion to transcriptional responses, with the larger dot representing 100%. For a more complete listing of regulated genes, see Dataset S2.

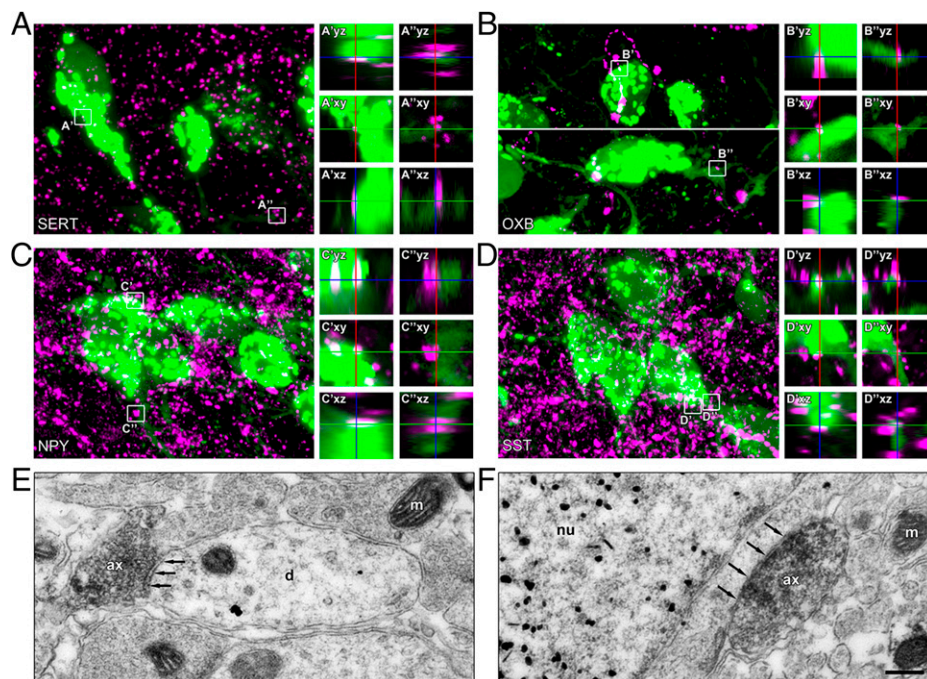


Fig. 3. Confocal and electron microscopic studies reveal the ligands of various estrogen-regulated neurotransmitter receptors in neuronal afferents to KP neurons. (A–D) Results of immunofluorescence studies on hypothalamic sections of OVX+Veh KP-Cre/ZsGreen mice confirm the presence of the serotonergic marker SERT (A) and the neuropeptides OXB (B), NPY (C), and SST (D) in axosomatic and/or axodendritic afferents (magenta) to MBH KP neurons (natural green color of ZsGreen-tagged cells). Low-power images represent confocal z-stacks. (Insets) Orthogonal views (z axis) of the neuronal contacts illustrate the absence of gaps between the juxtaposed profiles in single optical slices. Regulation of receptor transcripts for serotonin, OXB, NPY, and SST supports the concept that all of these transmitters contribute to the estrogen-dependent afferent control of KP neuron functions. (E and F) Electronmicroscopic studies confirm the presence of synaptic specializations (arrows) between SST-immunoreactive axons (ax) labeled with nickel-diaminobenzidine and tdTomato-immunoreactive KP neurons (silver-intensified gold nanoparticles) of transgenic mice. Synapses are present both on the dendrites (d; E) and the cell bodies (F) of KP neurons. Note in F that tdTomato fills the nucleus (nu) of the labeled KP neuron. m, mitochondrion. Scale bar: 10 μ m (A–D), 4 μ m (Insets), and 270 nm (Electron Micrographs). See also *SI Appendix, Table S1*.

The Estrogen-Regulated Transcriptome of ARC KP Neurons May Shed Light on the Pathomechanisms of Fertility Disorders and Designates Disease Gene Candidates.

We hypothesized that similarly to *Kiss1*, *Tac2*, and *Tacr3*, other transcripts heavily involved in reproductive regulation and disorders are 1) enriched in KP neurons versus their ARC environment, 2) expressed abundantly in KP cells (high counts per million [CPM]), and 3) regulated robustly (high $|\log_2FC|$) by E2. Searches of mouse (http://www.informatics.jax.org/vocab/mp_ontology) and human (<https://www.ebi.ac.uk/ols/ontologies/hp>) disease phenotype databases revealed that 7.1 ($n = 166$) and 1.8% ($n = 42$), respectively, of the 2,329 E2-regulated KP neuron transcripts can be linked to pubertal and reproductive disorders, including CHH (Fig. 5A). In total, 125 transcripts were expressed at mean CPM ≥ 100 , showed at least a threefold enrichment (in CPM) in KP neurons versus the ARC region, and showed at least a twofold up- or down-regulation by E2. The incidences of mouse and human disease genes increased to 20 ($n = 25$) and 8% ($n = 12$), respectively, by applying the above stringent selection criteria (color symbols in Fig. 5A). The list of the 125 candidate protein-coding genes was used for a gene-based burden analysis comparing the abundance of rare, likely pathogenic variants in a large cohort of CHH patients ($n = 337$) versus gnomAD control database (Fig. 5B). As expected, we observed an enrichment in known CHH genes such as *TAC3* ($P = 6.61E-08$), *TACR3* ($P = 1.01E-03$), and *KISS1* ($P = 6.15E-03$). Moreover, this analysis highlighted putative CHH-candidate genes like the low-density lipoprotein receptor-related protein 1B (*LRP1B*, $P = 3.14E-05$) and the voltage-gated calcium channel subunit alpha1 G (*CACNA1G*, $P = 1.84E-04$), a gene previously associated with spinocerebellar ataxia. Interestingly, the voltage-gated calcium

channel auxiliary subunit alpha2delta 1 (*CACNA2D1*, $P = 1.49E-03$) was also found among the enriched genes, suggesting an important role of L-type and T-type calcium channels in human reproduction. The emerging role of these candidate genes in the estrogen-dependent regulation of KP neurons and in CHH pathophysiology requires further clarification by basic research and clinical genetic studies.

Discussion

Technical Considerations. LCM is a high-precision approach to collect defined anatomical areas or subpopulations of tissue cells from histological sections under direct microscopic visualization. The regions of interest are selected and then dissected out with the aid of a laser beam for downstream applications, including transcriptomics. RNA-seq library preparation includes a DNase digestion step to eliminate nuclear DNA prior to reverse transcription of RNA. In this study, we developed two optimized protocols for tissue processing, LCM-based sample collection, RNA isolation, library preparation, and RNA-seq to achieve deep transcriptome profiling of the ARC and ARC KP (KNDy) neurons (*SI Appendix, Fig. S1A*). In both methods, the use of LCM allowed us to achieve a very precise histological sampling. This was reflected in 1) the homogeneous color blocks within heat maps and 2) the high number of transcripts that differed statistically ($p_{adj.} < 0.05$) between the OVX+Veh and OVX+E2 treatment groups. Manually microdissected ARC samples in a recent report (18) exhibited 132 estrogen-regulated transcripts at $FC > 1.5$ and $P < 0.05$, whereas 844 transcripts would correspond to the same cutoff criteria in our LCM-isolated ARC samples. We note that the two studies also differed in other technical

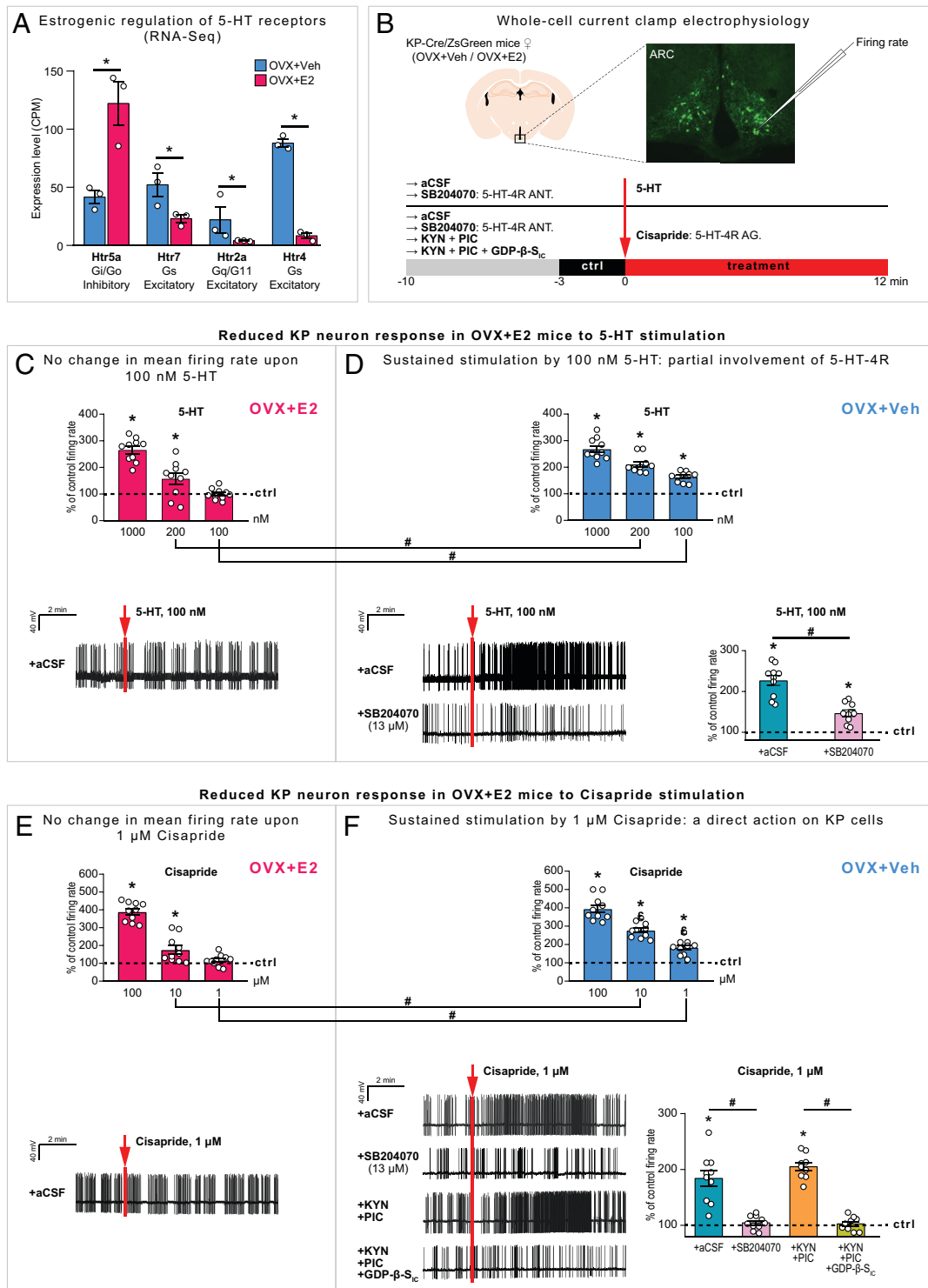
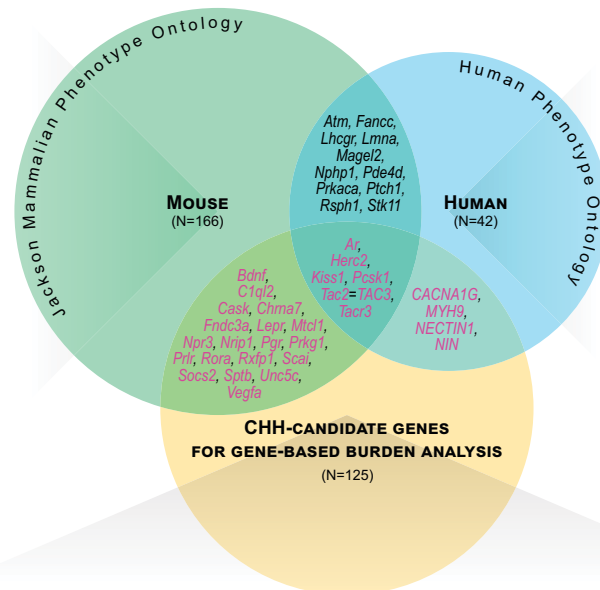


Fig. 4. Transcriptional changes of serotonin receptor isoforms cause reduced excitatory serotonergic neurotransmission to KP neurons in E2-treated OVX mice. (A) The 4-d E2 treatment of OVX mice (OVX+E2) causes up-regulation of the inhibitory *Htr5a* and down-regulation of the excitatory *Htr2a*, *Htr4*, and *Htr7* serotonin (5-HT) receptor isoforms in ARC KP neurons, leading to a prediction that 5-HT might stimulate KP neurons more efficiently in the OVX+Veh model. (B) Electrophysiological studies address the differential responsiveness of KP neurons from OVX+E2 versus OVX+Veh mice to decreasing doses of 5-HT or the selective 5-HT4R agonist (AG) Cisapride. (C–F) The highest doses of 5-HT (1,000 nM) and Cisapride (100 μ M) elicit similar increases in the mean firing frequency of KP neurons in OVX+E2 and OVX+Veh mice. In contrast, the OVX+Veh mouse model responds more to the medium and low doses (D vs. C; F vs. E). # $P < 0.05$ in OVX+Veh versus OVX+E2 model with ANOVA. (C and D) The 100-nM 5-HT, which has no effect in the OVX+E2 model (C), increases the mean firing frequency of KP cells in OVX+Veh mice to $163.6 \pm 6.10\%$ of the ctrl rate (D). Preincubation of slices with the selective 5-HT4R receptor antagonist (ANT) SB204070 (13 μ M) blunts this response (D), indicating the contribution of 5-HT4R isoform to the effect of 5-HT. (E and F) The 1- μ M dose of the selective 5-HT4R AG Cisapride has no significant effect on the mean firing rate of KP neurons in OVX+E2 mice (E; $116.6 \pm 10.06\%$ of ctrl; $P = 0.13$) but efficiently stimulates KP neuron firing in the OVX+Veh model (F; $184.1 \pm 13.64\%$ of ctrl; $P = 0.0002$). Cisapride acts selectively on 5-HT4R and, therefore, is ineffective in the presence of 13 μ M SB204070 (second trace in F). The effect on KP neurons is direct because it is preserved in the presence of the ionotropic glutamate and GABA_A receptor inhibitors KYN (2 mM) and PIC (100 μ M), respectively (third trace in F). Further, Cisapride is ineffective if the intracellular solution is supplemented with the G protein inhibitor GDP- β -S (2 mM; fourth trace in F). Scatter dot plots summarize the results obtained with different blockers. See also Dataset S3. * $P < 0.05$ versus ctrl with Student's *t* test. # $P < 0.05$ with ANOVA.

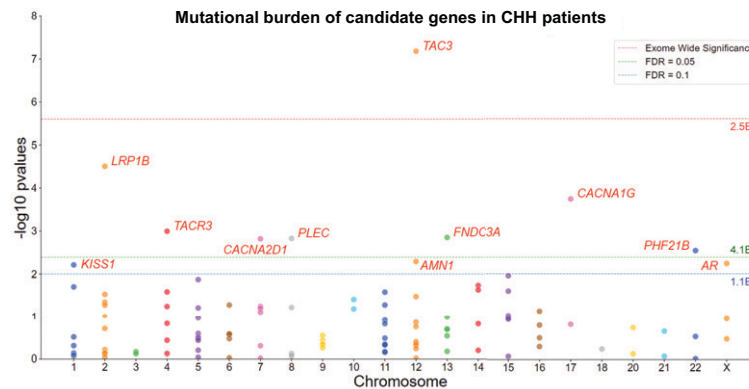
A *Abhd16a, Acd, Ace, Ache, Adams15, Adcy3, Adra1b, Akap12, Alk, Apc2, Arhgap1, Arsb, Asph, Atcay, Bbip1, Bbof1, Bcl2l1, Cacna1a, Cadm1, Cdkn1b, Cebp, Chst10, Chsy3, Cldn11, Cntnap1, Comt, Cpe, Cpeb3, Crem, Cttna2, Cux1, Ccs, Csf1r, Dcaf17, Dcx, Dkc1, Dmd, Eda, Egr1, Egr4, Ehd4, Elavl4, Emc10, Epb41l2, Esr1, Etv5, Fbxo7, Fkbp4, Fndc9, Gabbr1, Gabre, Gadd45g, Galnt3, Glib1, Gnao1, Golga3, Gorasp2, Gpd2, Grin1, Gtf2i, Hdac2, Hip1, Hspa4l, Hydin, Iqub, Irs4, Jade1, Jag2, Jund, Katnal1, Kif19a, Kl, Kmt2e, L1cam, Lgr4, Lpin1, Lsm14b, Mad2l2, Man2a2, Map1b, Marcks1, Mfge8, Mgat2, Mkm2, Msi2, Myo6, Nhlh2, Npr2, Nr2c2, Nsun2, Nxp1, Osbp2, Pascin1, Pcsk2, Pdgfb, Pgap1, Plekha1, Pomgnt1, Ppp2r5c, Prkce, Prkca, Ptipj, Qk, Rad18, Rappgef6, Rdx, Relb, Reln, Rhobtb3, Sec23ip, Selenop, Shank1, Slk3, Smarca2, Sms, Snap25, Sox3, Spag9, Sulf2, Tdrd7, Tdrkh, Tekt4, Tgfb3, Tns1, Tpst1, Trpc5, Vasn, Vgf, Vipr2, Zfp318*



BCSL1, CHRM3, DNAH9, DUSP6, FGFR1, FMR1, GNAS, GUCY1A1, LAS1L, LMNB1, NDN, PROK2, RTN2, SEMA3A, SIL1, STAR, TBL1X, TTC12, TTC8, VWF, WNT4

Akap13, Amn1, Amot1, Angptl2, Aqp5, Arvcf, Atp11a, Cacna1h, Cacna2d1, Cdh11, Cdh8, Cdkl5, Cers6, Cntnap5, Col24a1, Col4a2, Cxadr, Csm2d3, Dip2b, Dscam, Dscam1l, Epb41l4a, Fam135b, Fgf14, Fosl2, Galnt6, Gdpc2, Ghr, Glce, Gramd1b, Greb1, Grm7, Hcn1, Hivp1, Hmnc2, Hs3st5, Htr5a, Igf1, Igfbp1, Itgb1, Kcna4, Kcnk10, Kcnt1, Kctd4, Lamb1, Lrp1b, Mad2l1, Mark1, Mcf2l, Mctp1, Me3, Med13l, Mterf4, Nell1, Nfatc2, Npy1r, Nr4a2, Nr5a2, Nup205, Osbp3, Parp8, Pcdh11x, Pdyn, Phf21b, Phldb1, Plec, Plekha5, Ptchd1, Ptpru, Rai14, Rbms3, Sema5a, Serinc5, Shisa6, Slc38a3, Smoc2, Sned1, Sorcs1, Sox11, Spon1, Sv2c, Tgfb3, Thsd7a, Tmem131l, Tmem132b, Tmem25, Tmem266, Tmtc4, Tnxb, Tp53inp1, Tn, Ugcg, Unc13b, Xylt1, Zc3h12c

B



Causative genes and new putative CHH-candidate genes identified by gene-based burden analysis comparing CHH patients and controls

Ensembl transcript ID	HGNC symbol	Gene name	Gene MIM number	Human phenotype (Inheritance)	Phenotype MIM number	Enrichment p-value
ENST00000458521	TAC3	Neurokinin B	162330	Hypogonadotropic hypogonadism 10 with or without anosmia (AR)	614839	6.61E-08*
ENST00000389484	LRP1B	Low density lipoprotein receptor-related protein 1B	604065	-	-	3.14E-05*
ENST00000359106	CACNA1G	Calcium channel, voltage-dependent, T-type, alpha-1G subunit	608766	Spinocerebellar ataxia 42 (AD)	616795, 618067	1.84E-04*
ENST00000304883	TAC3	Neurokinin B receptor	162332	Hypogonadotropic hypogonadism 11 with or without anosmia (AR)	614840	1.01E-03*
ENST00000492622	FND3A	Fibronectin type III domain-containing protein 3A	615794	-	-	1.41E-03*
ENST00000322810	PLEC	Plectin	601282	Epidermolysis bullosa simplex (AR)	616487	1.49E-03*
ENST00000356860	CACNA2D1	Calcium channel, voltage-dependent, alpha-2/delta subunit 1	114204	-	-	1.52E-03*
ENST00000313237	PHF21B	PHD finger protein 21B	616727	-	-	2.88E-03*
ENST00000281471	AMN1	Antagonistic of mitotic exit network 1 homolog	-	-	-	5.12E-03
ENST00000374690	AR	Androgen receptor	313700	Androgen insensitivity (XLR)	300068	5.74E-03
ENST00000367194	KISS1	Kiss1 metastasis suppressor	603286	Hypogonadotropic hypogonadism 13 with or without anosmia	614842	6.15E-03

Fig. 5. The E2-regulated KP neuron transcriptome may serve as a resource to discover new genes causing fertility disorders. (A) The 2,329 E2-regulated genes of ARC KP neurons overlap with the lists of genes proposed to cause reproductive disturbances in mice and/or humans, according to the Jackson Mammalian Phenotype Ontology (green circle) and the Human Phenotype Ontology (blue circle) databases. In total, 17 disease genes are shared between mice and humans in the Venn diagram. Information about the E2-dependent transcripts of ARC KP neurons may serve as an important resource to identify new genetic causes of reproductive disturbances, including CHH. Note that 125 out of the 2,329 regulated transcripts (in yellow circle) are enriched at least 3 times in ARC KP neurons versus the ARC region, are expressed abundantly in KP cells (mean CPM ≥ 100), and respond to E2 at $|\log_2FC| \geq 1.0$. Gene names in red show overlaps with known mouse or human disease genes. (B) Manhattan plot illustrates the results of gene-based burden analysis of the top 125 candidate genes in a cohort of CHH patients versus gnomAd controls. Dotted lines indicate the threshold for statistical significance after correction for multiple testing (red: exome wide Bonferroni correction, $n = 20,000$, $P < 2.5E-06$; green: 5% false discovery rate [FDR] threshold; blue: 10% FDR threshold). Table contains basic data of putative CHH-candidate genes. Asterisks indicate enrichment P values below the 0.05% FDR threshold.

parameters, including steroid treatments, which could also contribute to partly different outcomes. A further methodological consideration relates to the choice of using LCM-isolated and pooled neurons in our study, as opposed to dispersed single cells in recent Drop-seq experiments on rodent hypothalamus (12, 13). These two sampling methods differ basically in their goals as well as in advantages and drawbacks. The LCM-based sample collection from pooled KP neurons ensured tens of thousands of identified transcripts, whereas reaching the same sequencing depth is beyond the goal of single-cell (e.g., Drop-seq) experiments in which tens of thousands of living cells are dispersed and then analyzed in the same sequencing run to identify clusters with identical gene expression properties (19). Accordingly, earlier Drop-seq studies of the hypothalamus (13) and its ARC region (12) were able to identify basic cell-type-specific transcriptional features of KNDy neurons, with intrinsic compromises in depth of sequencing. A critical advantage of LCM is the snapshot from a given functional status when the mice are killed, whereas the lengthy cell isolation process of Drop-seq and other single-cell techniques (19) may allow unwanted transcriptional changes to occur. This problem persists if living fluorescent neurons are isolated via fluorescence-activated cell sorting for sequencing. The RiboTag technique (20), which allows the selective isolation of actively translated mRNAs from a given cell population, offers an elegant alternative to our LCM-based cell harvesting approach, and it was used recently to identify estrogen-regulated transcripts of the preoptic (RP3V) KP neuron population (10). It has to be recognized that harvesting KP neurons with LCM has potential disadvantages as well. The transcriptomic information obtained from pooled neurons characterizes a mixed-cell population (~300 neurons in our study) instead of individual isolated cells, leaving possible heterogeneity of KP neurons unexplored. Another technical pitfall is some unavoidable sample contamination from surrounding tissues, which can be reduced using thin sections (12 μm in our study). Although some low-CPM transcripts identified in KP neurons may still represent false detection, we argue that the strict statistical criteria (*p*.adj. < 0.05) we applied ensure that the majority of changes reflect E2-dependent regulation within KP neurons.

Animal Models. In our study, we aimed to identify the E2-dependent transcripts of the ARC and its KP neurons. Our decision to use nonphysiological animal models to this goal relies on three main arguments. 1) Milder transcriptional effects of physiological E2 fluctuations across the estrus cycle would be much more difficult to identify as significant. 2) Transcriptomic snapshots from normal cycling animals would be impossible to interpret because of the different expression dynamics of E2-dependent transcripts. For example, some transcriptional responses to the high proestrus E2 levels might persist through estrus when serum E2 levels are at their nadir, whereas others could have already waned. Furthermore, ovarian progesterone dynamics would complicate the interpretation of estrogen effects based on the gene expression profile of intact females. 3) Surgical OVX and the subsequent treatment of OVX mice with exogenous E2 or vehicle generate two easily reproducible animal groups with low biological variations and high group homogeneity. Young female mice from mixed cycle phases contain 2.7 pg/mL serum E2 (Diestrus: ~6 pg/mL; Proestrus: ~8 pg/mL; Estrus: <0.3 pg/mL; Metestrus: ~0.5 pg/mL, as determined by gas chromatography-tandem mass spectrometry [GC-MS/MS]) (11). Thus, the 7.59 ± 0.74 pg/mL serum E2

cc. we detected in OVX+E2 test mice falls in the physiological range, which characterizes cycling female mice at times of strong negative feedback. We note that the real serum E2 concentration in this OVX+E2 model might be somewhat lower due to the previously noted serum matrix effect (21) that we also detected. Accordingly, the $1.73 + 0.34$ pg/mL E2 concentration this kit detected in our OVX+Veh mice is likely an overestimate because OVX mice are known to contain E2 below the 0.3 pg/mL detection threshold of GC-MS/MS (11). Despite these technical issues, a systematic comparison of nine commercial enzyme immunoassay kits showed that the CalBiotech Kit ES180S-100 kit is still the only one available currently that shows good E2 parallelism to the standard curve as well as accuracy versus the gold standard GC-MS/MS technique (21).

It is reasonable to speculate that the estrogen-dependent ARC and KP neuron transcriptomes identified in this study show physiological fluctuations in intact female mice according to cyclic changes in E2 negative feedback. However, the expression level of individual transcripts in our OVX+E2 model may not necessarily reflect the transcriptional landscape of intact diestrus/proestrus animals. We propose that the extended 4-d E2 treatment of OVX mice may be clinically relevant to chronic estrogen exposure with relative progesterone deficiency, which is a common perimenopausal pathology, whereas transcriptomes of the OVX+Veh model may mimic the gene expression status of the ARC and its KP neurons following the loss of estrogens in postmenopausal women.

Comparison with Earlier Studies of the ARC. Earlier RNA-seq experiments have already addressed the estrogen responsiveness of the ARC transcriptome (18). This study used OVX wild-type mice, ER α knockout mice, and mice containing ER α with a mutated DNA binding domain to distinguish among ER α -mediated, estrogen response element (ERE)-dependent, and ER α -independent E2 signaling, respectively. The number of significant changes (at *P* < 0.05 and FC > 1.5) occurred to 132, 35, and 22 transcripts, respectively, in these three cases. The ARC of OVX+E2 mice in our study reproduced many (e.g., *Stc1*, *Mfge8*, *Pcdh20*, *Crabp1*, *Wnt4*, *Pou3f1*, *Gpr88*), but not all (e.g., *Mgp*, *Erp27*, *Msx1*, *Pou2f1*, *Olig2*, *Msx1*, *Gfap*), of the above 132 transcriptional changes. In addition, the ARC transcriptome of our OVX+E2 mice exhibited significant changes not reported by these investigators. Altogether, we found 4,039 transcripts at *P* < 0.05 and 2,117 transcripts at *p*.adj. < 0.05 that were expressed differentially in the two treatment groups. Out of these, 844 and 483 changed more than 1.5 times at *P* < 0.05 and *p*.adj. < 0.05, respectively. The much higher number of regulated transcripts identified in our study may partly reflect the use of different methods, including the very precise LCM-based tissue collection. Differences in the estrogen treatment of OVX mice could also contribute to the partly different transcriptional responses and gene regulation dynamics; our study used a chronic 4-d E2 substitution of OVX mice via silastic capsule implants, whereas Yang and colleagues (18) applied two estradiol benzoate injections in oil to OVX mice 24 and 48 h before sacrifice, respectively. While our studies focused on the regulation of KNDy neurons, the comparative analysis of the E2-dependent ARC and KP neuron transcriptome databases will be very useful in future studies to identify transcripts that are regulated specifically within KP neurons. Among these, newly identified peptide cotransmitters of KNDy neurons include *Vgf* and *Nms*, and regulated receptors expressed at higher levels (CPMs) in KP neurons than in the ARC include *Npy4r*, *Ghsr*, *Lepr*, and *Prhr*, among others. It

is important to note that KP neurons are not the only estrogen-dependent cell type in the ARC, as revealed by the altered expression of neurotensin (*Nts*), SST (*Sst*), agouti-related peptide (*AgRP*), prepronociceptin (*Pnoc*), preproenkephalin (*Penk*), and CART prepropeptide (*Cartpt*) in the ARC of our OVX+E2 model. The above and similar E2-dependent transcripts that are not regulated and enriched within KP cells contribute to our understanding of the estrogenic control of non-KP neurons, potentially including currently unknown ARC neuron populations.

Differential Regulation of the Two KP Neuron Populations by E2.

This comprehensive study identifies the estrogen-sensitive transcripts of ARC KP neurons with deep transcriptome profiling. A handful of transcriptional changes including the estrogenic down-regulation of *Kiss1*, *Tac2*, and *Tacr3* were previously known from in situ hybridization experiments (22), whereas the majority of the 2,329 regulated transcripts represent discoveries. While we did not address the estrogenic regulation of RP3V KP neurons implicated in positive E2 feedback, a recent RNA-seq study based on the RiboTag technology managed to identify 683 E2-dependent changes in the transcriptome of RP3V KP neurons at $P < 0.05$ (10). Although it is not clear how many of these changes satisfy the more stringent statistical criteria of $p_{adj.} < 0.05$, the relatively small number of responsive transcripts raises the possibility that the transcriptome of RP3V KP neurons is less responsive to E2 treatment than the ARC KP neuron transcriptome, the latter of which exhibited 2,329 changes at $p_{adj.} < 0.05$ and 4,391 changes at $P < 0.05$. Not too surprisingly, the neuroactive ligand-receptor interaction KEGG pathway was altered significantly in both KP cell types, with 57 changes in ARC and 32 reported changes in RP3V KP neurons. Comparison of the E2-dependent genes identified in the two studies reveals interesting regulatory similarities as well as differences between the two KP neuron populations. Transcripts regulated in the same direction in RP3V and ARC KP neurons include *Pgr*, *Pdyn*, *Vglut2*, and *Npy4r*. Many interesting examples also exist for an inverse regulation within the two KP cell groups (e.g., *Kiss1*, *Vgf*, *Gal*, and *Prlr*). Comparative analysis of regulatory patterns in the ARC and the RP3V KP neuron population may provide important insight into the regulatory mechanisms underlying negative and positive estrogen feedback. Immunohistochemical studies in the future will be used to investigate further the presence and estrogen-dependent regulation of neuropeptide cotransmitters (neuromedin S, VGF, galanin) in ARC KP neurons. Although our present study focused on the 2,329 E2-dependent transcripts of ARC KP neurons, we note that the full transcriptome contained 19,796 different transcripts at a mean CPM > 1 and 11,164 transcripts at a mean CPM > 10 . Many of these transcripts not shown here to be regulated by E2 might fulfill critical roles in KP neuron physiology.

Mechanisms Underlying the Transcriptional Changes. Multiple mechanisms that account for the altered gene expression profile of E2-treated OVX mice (23–25) are inseparable in our study. Classical genomic actions of E2 involve ligand binding to cytoplasmic ERs (ER α and ER β), which induces receptor dimerization and entry into the nucleus. The homo- or heterodimer complex binds to EREs in the promoter region of target genes and induces or represses transcription. It was estimated that the mouse and human genomes contain $\sim 70,000$ such EREs (26). Primary responsive genes may also lack any ERE-like sequence and require a DNA-binding transcription cofactor. In this indirect (tethered) genomic signaling mechanism, ERs participate in

protein-protein interactions to modulate the function of other response elements and TFs, many of which were expressed in KP neurons (e.g., *Sp1*, *Nfkb1*, *Cebpb*, *Stat5a*, and *Stat5b*). Unknown fractions of classic ERs may be membrane bound to mediate rapid estrogen effects. This pool in the proximity of the plasma membrane can be associated with the scaffold protein caveolin-1 or Src, Ras, and PI3 kinases. Upon binding E2, various signaling cascades can be activated to generate calcium currents, cyclic adenosine monophosphate, or inositol phosphate or to stimulate protein kinases (25). Estrogens may also act via the G protein-coupled ER 1 (*Gper1*, a.k.a. *Gpr30*) (27). However, *Gper1* was expressed only at extremely low levels in the ARC and in KP neurons (mean CPM = 2.2 and 2.5, respectively), suggesting that its contribution to the observed transcriptional changes is negligible. There is a large body of evidence that estrogens regulate mitochondrial functions (28).

In addition to the above direct effects, many changes we observed in this study could be consequences of indirect estrogen actions on neuronal, glial, or endothelial cell types communicating with the ARC and with KP neurons. Detailed analysis of mechanisms regulating individual genes would not be possible within the limits of this article.

Estrogenic Regulation of TFs. RNA-seq results revealed that *Esr1* is one of the most abundant TFs in KP neurons conveying robust estrogen dependence to these neurons. Strikingly, E2 treatment of OVX mice altered mRNA expression of 109 TFs. The transcription of *Ar*, *Egr1*, *Fos*, *Fosb*, *Junb*, *Nr4a1*, and *Sox3* was suppressed by E2, whereas the well-known estrogen target *Pgr* showed a strong stimulatory response. Transcriptional regulation of TFs could contribute significantly to secondary changes in the expression profile and functions of KP cells.

Regulatory RNAs in ARC KP Neurons. In addition to five miRNAs, at least 60 lncRNAs were regulated by E2 in KP neurons. These transcripts are longer than 200 nucleotides, with no or only limited protein-coding capability, and they are categorized as long intronic ncRNAs, long intergenic ncRNAs, circular RNAs, and natural antisense transcripts. Most lncRNAs act in the cell nucleus as molecular scaffolds to assist in alternative splicing, chromatin structure modification, and other biological processes. In the cytoplasm, lncRNAs regulate translation, promote or inhibit mRNA degradation, and function as miRNA sponges (29, 30). The critical role of lncRNAs is increasingly recognized in a variety of biological processes and in the pathophysiology of cancer initiation, development, and progression (31). These lncRNAs are also emerging as important determinants of nuclear hormone receptor action (29, 30). For example, MALAT1, which was expressed abundantly but not regulated in KP cells, associates with both ER α and ER β at the chromatin level, and E2 treatment of prostate organotypic slice cultures decreases MALAT1 recruitment to chromatin (32). MIAT was regulated robustly by E2 in KP cells, similarly to previous observations obtained in ER-positive breast cancer cells (33). The crosstalk among lncRNAs, estrogens, and ERs may have wider implications in sex steroid signaling, as indicated by the estrogenic regulation of 60 lncRNAs within KP neurons. The importance of these changes in the regulation of sex steroid feedback to the neuroendocrine hypothalamus requires clarification.

Functional Consequences of E2 Treatment on Neurotransmitter Signaling to ARC KP Neurons. ORA unveiled the significant alteration of 83 KEGG pathways, including the mitogen-activated protein kinase-, cyclic adenosine monophosphate-, PI3K-Akt-,

Calcium-, cyclic guanosine monophosphate-dependent protein kinase-, and 5' adenosine monophosphate-activated protein kinase-signaling pathways. Future research will need to investigate the functional consequences of these changes, which would be impossible to discuss thoroughly in this manuscript. In our study, we paid special attention to the neuroactive ligand-receptor interaction pathway with 57 E2-regulated transcripts, which indicated that E2 treatment profoundly alters neuropeptidergic, GABAergic, glutamatergic, dopaminergic, cholinergic, and serotonergic signaling to ARC KP neurons. Using neuroanatomical approaches, we confirmed that various neuropeptide receptor ligands (OX B, SST, NPY) and serotonin are present in neuronal afferents to KP neurons. In the case of SST, it would be difficult to speculate about the physiological consequences of the opposite regulation of *Sstr2* and *Sstr3* (induction of *Sstr2* and inhibition of *Sstr3* by E2), both of which encode receptors that inhibit adenylyl cyclases. Similar problems hinder the physiological interpretation of regulatory changes shown by the three distinct *Npyr* transcripts (down-regulation of *Npy1r* and *Npy5r* vs. up-regulation of *Npy4r*), in which case the encoded receptors can even have multiple physiological ligands (NPY/PYY/PP). In contrast, changes of all four regulated serotonin receptors (estrogenic up-regulation of the inhibitory *Htr5a* and down-regulation of the excitatory *Htr2a*, *Htr7*, and *Htr4*) allowed us to hypothesize reduced serotonergic stimulation of KP neurons in the OVX+E2 model, also in accordance with the reduced function of the serotonergic synapse pathway predicted by SPIA. Our experiments using slice electrophysiology confirmed the hypothesis that serotonin exerts reduced excitatory action on KP neurons in the OVX+E2 mouse model, and this reduction is partly due to decreased excitatory signaling on serotonin receptor 4. A large body of evidence indicates the involvement of serotonergic mechanisms in the estrogen-dependent control of the pulsatile and surge modes of LH release (for a review, see ref. 16). The high rate of LH release is inhibited by serotonin in OVX rats, whereas LH secretion is stimulated in rats pretreated with E2. Counterintuitively, ARC KP neurons in our electrophysiological studies gave higher responses to serotonin in slices of OVX+Veh mice, which suggests multiple hypothalamic sites and mechanisms for the in vivo reproductive actions of serotonin. OVX female rats were reported to show a morning/afternoon oscillatory pattern in serotonin metabolism in several brain areas associated with the control of LH secretion. This pattern is modulated by E2 in a way that the peak serotonergic activity coincides with the induced afternoon LH surge (16). ARC KP neurons contribute to the reproductive effects of serotonin. In male rats, intracerebroventricular serotonin injection increases hypothalamic *Kiss1* expression encoding KP (34). Dysregulation of NKB secretion from ARC KP neurons plays an important role in postmenopausal hot flashes (35). Interestingly, selective serotonin reuptake inhibitors are among the most efficient non-hormonal treatment options for hot flashes (36).

Putative Involvement of Estrogen-Regulated Genes in Human Fertility Disorders. Several E2-regulated transcripts enriched in KP neurons are known for their role in the control of reproduction. These include *Kiss1*, *Tac2*, *Tacr3*, and *Esr1*, among others that could also be found in the Jackson Mammalian Phenotype Ontology and the Human Phenotype Ontology databases. We propose that such genes can be critical regulators of human fertility, and their mutations may underlie currently unexplained cases of CHH. To facilitate future genetic screening of patient databases, we have generated a list rich in putative disease genes using stringent selection criteria (at least threefold enrichment

in KP neurons vs. the ARC region, at least twofold change ($|\log_2FC| \geq 1.0$) in response to E2, and mean CPM ≥ 100 within KP neurons). This strategy enhanced the incidence of known murine disease genes from 7.1 to 20.0% and the incidence of known human disease genes from 1.8 to 8.0% in the list. This enrichment made it very likely that the incidences of currently unknown disease genes were also increased. This hypothesis is supported by the gene-based burden analysis of the top 125 candidate genes from our expression study comparing a large cohort of CHH patients versus gnomAD controls. Indeed, patients showed enrichments in rare transcript variants of several known CHH genes such as *TAC3*, *TACR3*, and *KISS1* together with putative CHH-candidate genes, including two members of the voltage-gated calcium channels family. Although results of this preliminary burden analysis do not necessarily indicate a causal relationship between the rare variants and CHH, they suggest that the list of the heavily estrogen-dependent KP neuron transcripts may become an important resource for the discovery of new genes responsible for human reproductive phenotypes.

Conclusions. According to the prevailing view, ARC KP (KNDy) neurons are key regulators of pulsatile GnRH secretion via KP/KP receptor signaling on the preterminal “dendrons” of hypophysiotropic GnRH processes. This signaling is critically influenced by the negative feedback effects of the ovarian sex steroid E2 (1, 2). Molecular mechanisms underlying this feedback are only poorly understood. E2 uses direct and indirect pathways to alter the gene expression profile of KP neurons. RNA-seq studies of the ARC identified changes in neuropeptide genes that are enriched in non-KP cells. Altered *Agrp*, *Nts*, and *Sst* expression may act transsynaptically to influence KP neurons that express *Mc3r*, *Ntsr2*, and *Sstr2/Sstr3* receptors, respectively, according to results of our KP neuron transcriptomics. Further actions of E2 outside the ARC may also alter the gene expression profile of KP neurons via indirect transsynaptic actions, whereas our RNA-seq studies found no solid evidence for a putative glial/endothelial involvement in indirect E2 actions upon KP cells. Transcriptional changes within KP neurons include the reduced expression of nearly all neuropeptide cotransmitters (e.g., *Kiss1*, *Tac2*, *Pdyn*, *Gal*, *Vgf*) and secretory proteins (e.g., *Chga*, *Chgb*, *Scg3*) colocalized with KP. In contrast, the level of the *Slc17a6* transcript, which encodes VGLUT2 and confers a glutamatergic phenotype onto KNDy neurons (37), increased considerably. E2 changed the expression of various nuclear (e.g., *Esr1*, *Ar*, *Pgr*) and membrane (e.g., *Prlr*, *Ghnr*, *Lepr*) hormone receptors, receptors for classic (e.g., *Adra1a*, *Htr4*) and neuropeptide (e.g., *Hcr2*, *Npy1r*, *Tacr3*) transmitters, and ion channels and regulated a variety of biological processes, including transcription, mitochondrial and ribosomal functions, ubiquitination, autophagy, and synaptic plasticity. The surprisingly large number of E2-regulated lncRNAs opens an area in sex steroid research. The comprehensive characterization of the estrogen-dependent KP neuron transcriptome in mice also has important clinical implications for the estrogenic regulation of the human hypothalamus during the menstrual cycle and for the putative molecular consequences of postmenopausal estrogen deficiency.

Materials and Methods

A detailed description of methodologies—including the use of transgenic mouse strains, estrogen treatment, transcriptomic studies, immunohistochemical experiments, confocal and electron microscopic studies, slice electrophysiology, and gene-based burden analysis—is provided in [SI Appendix, Materials and Methods](#).

Data Availability. RNA-seq files have been deposited in BioProject on December 20, 2020, with the accession number [PRJNA686688](https://www.ncbi.nlm.nih.gov/bioproject/PRJNA686688) (38). Scripts are available at GitHub at https://github.com/solymosin/PRJNA686688_ms_codes (39).

ACKNOWLEDGMENTS. The research leading to these results has received funding from the National Science Foundation of Hungary (Grants: K128317 and K138137 to E.H. and PD134837 to K.S.) and the Hungarian Brain Research Program (Grant: 2017-1.2.1-NKP-2017-00002 to E.H.). The authors thank Drs. P. Ciofi (INSERM, Bordeaux, France), I. Merchenthaler (University of Maryland, Baltimore, MD), and C. Fekete (Institute of Experimental Medicine, Budapest, Hungary) for kindly providing SST, NPY, and tdTomato antibodies, respectively, for these studies.

Author affiliations: ^aLaboratory of Reproductive Neurobiology, Institute of Experimental Medicine, Budapest 1083, Hungary; ^bJános Szentágotthai Doctoral School of Neurosciences, Semmelweis University, Budapest 1085, Hungary; ^cLaboratory of Endocrine Neurobiology,

1. S. M. Moenter, M. A. Silveira, L. Wang, C. Adams, Central aspects of systemic oestradiol negative- and positive-feedback on the reproductive neuroendocrine system. *J. Neuroendocrinol.* **32**, e12724 (2020).
2. A. E. Herbison, A simple model of estrous cycle negative and positive feedback regulation of GnRH secretion. *Front. Neuroendocrinol.* **57**, 100837 (2020).
3. N. E. Rance, N. T. McMullen, J. E. Smialek, D. L. Price, W. S. Young III, Postmenopausal hypertrophy of neurons expressing the estrogen receptor gene in the human hypothalamus. *J. Clin. Endocrinol. Metab.* **71**, 79–85 (1990).
4. N. E. Rance, W. S. Young III, Hypertrophy and increased gene expression of neurons containing neurokinin-B and substance-P messenger ribonucleic acids in the hypothalamus of postmenopausal women. *Endocrinology* **128**, 2239–2247 (1991).
5. E. Hrabovszky *et al.*, Sexual dimorphism of kisspeptin and neurokinin B immunoreactive neurons in the infundibular nucleus of aged men and women. *Front. Endocrinol. (Lausanne)* **2**, 80 (2011).
6. A. M. Rometo, S. J. Krajewski, M. L. Voytko, N. E. Rance, Hypertrophy and increased kisspeptin gene expression in the hypothalamic infundibular nucleus of postmenopausal women and ovariectomized monkeys. *J. Clin. Endocrinol. Metab.* **92**, 2744–2750 (2007).
7. E. Hrabovszky *et al.*, Substance P immunoreactivity exhibits frequent colocalization with kisspeptin and neurokinin B in the human infundibular region. *PLoS One* **8**, e72369 (2013).
8. M. A. Mittelman-Smith *et al.*, Arcuate kisspeptin/neurokinin B/dynorphin (KNDy) neurons mediate the estrogen suppression of gonadotropin secretion and body weight. *Endocrinology* **153**, 2800–2812 (2012).
9. X. Liu *et al.*, Highly redundant neuropeptide volume co-transmission underlying episodic activation of the GnRH neuron dendron. *eLife* **10**, e62455 (2021).
10. S. B. Z. Stephens, A. S. Kauffman, Estrogen regulation of the molecular phenotype and active transcriptome of AVPV kisspeptin neurons. *Endocrinology* **162**, bqab080 (2021).
11. M. E. Nilsson *et al.*, Measurement of a comprehensive sex steroid profile in rodent serum by high-sensitive gas chromatography-tandem mass spectrometry. *Endocrinology* **156**, 2492–2502 (2015).
12. J. N. Campbell *et al.*, A molecular census of arcuate hypothalamus and median eminence cell types. *Nat. Neurosci.* **20**, 484–496 (2017).
13. R. Chen, X. Wu, L. Jiang, Y. Zhang, Single-cell RNA-seq reveals hypothalamic cell diversity. *Cell Rep.* **18**, 3227–3241 (2017).
14. S. Schuierer *et al.*, A comprehensive assessment of RNA-seq protocols for degraded and low-quantity samples. *BMC Genomics* **18**, 442 (2017).
15. S. D. Sullivan, L. C. Howard, A. H. Clayton, S. M. Moenter, Serotonergic activation rescues reproductive function in fasted mice: Does serotonin mediate the metabolic effects of leptin on reproduction? *Biol. Reprod.* **66**, 1702–1706 (2002).
16. M. L. Vitale, S. R. Chiochio, Serotonin, a neurotransmitter involved in the regulation of luteinizing hormone release. *Endocr. Rev.* **14**, 480–493 (1993).
17. S. de Croft *et al.*, Spontaneous kisspeptin neuron firing in the adult mouse reveals marked sex and brain region differences but no support for a direct role in negative feedback. *Endocrinology* **153**, 5384–5393 (2012).
18. J. A. Yang, H. Stires, W. J. Belden, T. A. Roeper, The arcuate estrogen-regulated transcriptome: Estrogen response element-dependent and -independent signaling of ER α in female mice. *Endocrinology* **158**, 612–626 (2017).
19. B. Vieth, S. Parekh, C. Ziegenhain, W. Enard, I. Hellmann, A systematic evaluation of single cell RNA-seq analysis pipelines. *Nat. Commun.* **10**, 4667 (2019).
20. E. Sanz *et al.*, Cell-type-specific isolation of ribosome-associated mRNA from complex tissues. *Proc. Natl. Acad. Sci. U.S.A.* **106**, 13939–13944 (2009).

Institute of Experimental Medicine, Budapest 1083, Hungary; ^dDepartment of Cellular and Network Neurobiology, Institute of Experimental Medicine, Budapest 1083, Hungary; ^eLaboratory of Integrative Neuroendocrinology, Institute of Experimental Medicine, Budapest 1083, Hungary; ^fCentre for Bioinformatics, University of Veterinary Medicine, Budapest 1078, Hungary; ^gDepartment of Physics of Complex Systems, Eötvös Loránd University, Budapest 1117, Hungary; ^hDepartment of Biochemistry and Molecular Biology, Faculty of Medicine, University of Debrecen, Debrecen 4032, Hungary; ⁱDepartment of Animal Biotechnology, Institute of Genetics and Biotechnology, Hungarian University of Agriculture and Life Sciences, Gödöllő 2100, Hungary; ^jService of Endocrinology, Diabetology, and Metabolism, Lausanne University Hospital, Lausanne 1011, Switzerland; ^kFaculty of Biology and Medicine, University of Lausanne, Lausanne 1005, Switzerland; ^lCentre for Neuroendocrinology, University of Pretoria, Pretoria 0031, South Africa; ^mTranslational & Clinical Research Institute, University of Newcastle-upon-Tyne, Newcastle upon Tyne NE1 4EP, United Kingdom; ⁿDepartment of Endocrinology, Diabetes & Metabolism, Newcastle-upon-Tyne Hospitals, Newcastle upon Tyne NE1 4LP, United Kingdom; and ^oDepartment of Physiology, Development and Neuroscience, University of Cambridge, Cambridge CB2 3EG, United Kingdom

Author contributions: B.G., É.R., M.S., K.S., S.T., I.F., S.P., Z.S., L.B., Y.Z., A.M., N.P., W.H.C., and E.H. designed research; B.G., É.R., M.S., K.S., S.T., I.F., V.C., S.H.T., Z.B., Y.R., N.S., S.P., Z.S., L.B., Y.Z., A.M., N.P., S.M.M., and E.H. performed research; R.C.A., R.P.M., and R.Q. contributed new reagents/analytic tools; B.G., É.R., M.S., K.S., S.T., I.F., V.C., N.S., S.P., Z.S., L.B., Y.Z., A.M., N.P., and E.H. analyzed data; and B.G., É.R., M.S., K.S., S.T., I.F., S.P., L.B., Y.Z., A.M., N.P., S.M.M., W.H.C., and E.H. wrote the paper.

21. D. J. Haisenleder, A. H. Schoenfelder, E. S. Marcinko, L. M. Geddis, J. C. Marshall, Estimation of estradiol in mouse serum samples: Evaluation of commercial estradiol immunoassays. *Endocrinology* **152**, 4443–4447 (2011).
22. V. M. Navarro *et al.*, Regulation of gonadotropin-releasing hormone secretion by kisspeptin/dynorphin/neurokinin B neurons in the arcuate nucleus of the mouse. *J. Neurosci.* **29**, 11859–11866 (2009).
23. R. O'Lone, M. C. Frith, E. K. Karlsson, U. Hansen, Genomic targets of nuclear estrogen receptors. *Mol. Endocrinol.* **18**, 1859–1875 (2004).
24. P. Vrtačník, B. Ostanek, S. Mencej-Bedrač, J. Marc, The many faces of estrogen signaling. *Biochem. Med. (Zagreb)* **24**, 329–342 (2014).
25. L. Björnström, M. Sjöberg, Mechanisms of estrogen receptor signaling: Convergence of genomic and nongenomic actions on target genes. *Mol. Endocrinol.* **19**, 833–842 (2005).
26. V. Bourdeau *et al.*, Genome-wide identification of high-affinity estrogen response elements in human and mouse. *Mol. Endocrinol.* **18**, 1411–1427 (2004).
27. A. K. Treen *et al.*, Divergent regulation of ER and kiss genes by 17 β -estradiol in hypothalamic ARC versus AVPV models. *Mol. Endocrinol.* **30**, 217–233 (2016).
28. C. M. Klinge, Estrogenic control of mitochondrial function and biogenesis. *J. Cell. Biochem.* **105**, 1342–1351 (2008).
29. S. Nanni *et al.*, Signaling through estrogen receptors modulates long non-coding RNAs in prostate cancer. *Mol. Cell. Endocrinol.* **511**, 110864 (2020).
30. R. Zhang, V. Wesевич, Z. Chen, D. Zhang, A. N. Kallen, Emerging roles for noncoding RNAs in female sex steroids and reproductive disease. *Mol. Cell. Endocrinol.* **518**, 110875 (2020).
31. V. R. Ramnarine *et al.*, The evolution of long noncoding RNA acceptance in prostate cancer initiation, progression, and its clinical utility in disease management. *Eur. Urol.* **76**, 546–559 (2019).
32. A. Aiello *et al.*, MALAT1 and HOTAIR long non-coding RNAs play opposite role in estrogen-mediated transcriptional regulation in prostate cancer cells. *Sci. Rep.* **6**, 38414 (2016).
33. Y. Li *et al.*, Long non-coding RNA MIAT is estrogen-responsive and promotes estrogen-induced proliferation in ER-positive breast cancer cells. *Biochem. Biophys. Res. Commun.* **503**, 45–50 (2018).
34. F. Mahmoudi, K. Haghghat Gollo, Influences of serotonin hydrochloride on *Adiponectin*, *Ghrelin* and *KiSS1* genes expression. *Galen Med. J.* **9**, e1767 (2020).
35. N. E. Rance, P. A. Dacks, M. A. Mittelman-Smith, A. A. Romanovsky, S. J. Krajewski-Hall, Modulation of body temperature and LH secretion by hypothalamic KNDy (kisspeptin, neurokinin B and dynorphin) neurons: A novel hypothesis on the mechanism of hot flashes. *Front. Neuroendocrinol.* **34**, 211–227 (2013).
36. H. D. Nelson *et al.*, Nonhormonal therapies for menopausal hot flashes: Systematic review and meta-analysis. *JAMA* **295**, 2057–2071 (2006).
37. P. Ciofi, D. Leroy, G. Tramu, Sexual dimorphism in the organization of the rat hypothalamic infundibular area. *Neuroscience* **141**, 1731–1745 (2006).
38. B. Göcz *et al.*, Data from "Transcriptome profiling of kisspeptin neurons from the mouse arcuate nucleus reveals new mechanisms in estrogenic control of fertility." BioProject. <https://www.ncbi.nlm.nih.gov/bioproject/?term=PRJNA686688>. Deposited 20 December 2020.
39. B. Göcz *et al.*, Data from "Transcriptome profiling of kisspeptin neurons from the mouse arcuate nucleus reveals new mechanisms in estrogenic control of fertility." GitHub. https://github.com/solymosin/PRJNA686688_ms_codes. Deposited 18 May 2022.